Title

A Design of Experiment (DoE) approach to optimise spray drying process conditions for the production of trehalose/leucine formulations with application in pulmonary delivery

Authors

Focaroli, S
Mah, PT
Hastedt, JE
et al.

Publication Date

2019-05-01

DOI

10.1016/j.ijpharm.2019.03.004

Peer reviewed

HHS Public Access

Author manuscript

Int J Pharm. Author manuscript; available in PMC 2020 May 01.

Published in final edited form as:

Int J Pharm. 2019 May 01; 562: 228–240. doi:10.1016/j.ijpharm.2019.03.004.

A Design of Experiment (DoE) approach to optimise spray drying process conditions for the production of trehalose/leucine formulations with application in pulmonary delivery

S. Focaroli[a], **P.T. Mah**[a], **J. E. Hastedt**[b], **I. Gitlin**[c], **S. Oscarson**[d], **J.V. Fahy**[c], and **A.M. Healy**[a,e]

[a]School of Pharmacy and Pharmaceutical Sciences, Panoz Insitute, Trinity College Dublin, Dublin 2, Ireland [b]JDP Pharma Consulting, LLC, PO Box 1127, San Carlos, California, United States [c]Division of Pulmonary and Critical Care Medicine, Department of Medicine and Cardiovascular Research Institute, Health Sciences East, UCSF, 513 Parnassus Avenue, San Francisco, CA, United States [d]Centre for Synthesis and Chemical Biology, School of Chemistry and Chemical Biology, University College Dublin, Belfield, Dublin 4, Ireland [e]Synthesis and Solid State Pharmaceutical Centre, Trinity College Dublin, Dublin 2, Ireland

Abstract

The present study evaluates the effect of L-leucine concentration and operating parameters of a laboratory spray dryer on characteristics of trehalose dry powders, with the goal of optimizing production of these powders for inhaled drug delivery. Trehalose/L-leucine mixtures were spray dried from aqueous solution using a laboratory spray dryer. A factorial design of experiment (DoE) was undertaken and process parameters adjusted were: inlet temperature, gas flow rate, feed solution flow rate (pump setting), aspiration setting and L-leucine concentration. Resulting powders were characterised in terms of particle size, yield, residual moisture content, and glass transition temperature. Particle size was mainly influenced by gas flow rate, whereas product yield and residual moisture content were found to be primarily affected by inlet temperature and spray solution feed rate respectively. Interactions between a number of different process parameters were elucidated, as were relationships between different responses. The leucine mass ratio influenced the physical stability of powders against environmental humidity, and a high leucine concentration (30% w/w) protected amorphous trehalose from moisture induced crystallization. High weight ratio of leucine in the formulation, however, negatively impacted the aerosol performance. Thus, in terms of L-leucine inclusion in a formulation designed for pulmonary delivery, a balance needs to be found between physical stability and deposition characteristics.

Corresponding author: Anne Marie Healy School of Pharmacy and Pharmaceutical Sciences, Trinity College, University of Dublin, Dublin 2, Ireland. Phone: +353-1-8961444 healyam@tcd.ie.

Author Contribution Statement.

Focaroli S. and Healy A.M. conceived and planned the experiments. Focaroli S. and Mah P.T carried out the experiments. Healy A. M., J. E., Gitlin I., Oscarson S., Fahy, J.V. obtained and supervised the findings of this work. Focaroli S. took the lead in writing the manuscript. All authors contributed to the interpretation of the results and provided critical feedback and helped shape the research, analysis and manuscript. Healy A.M. supervised the project.

Graphical Abstract

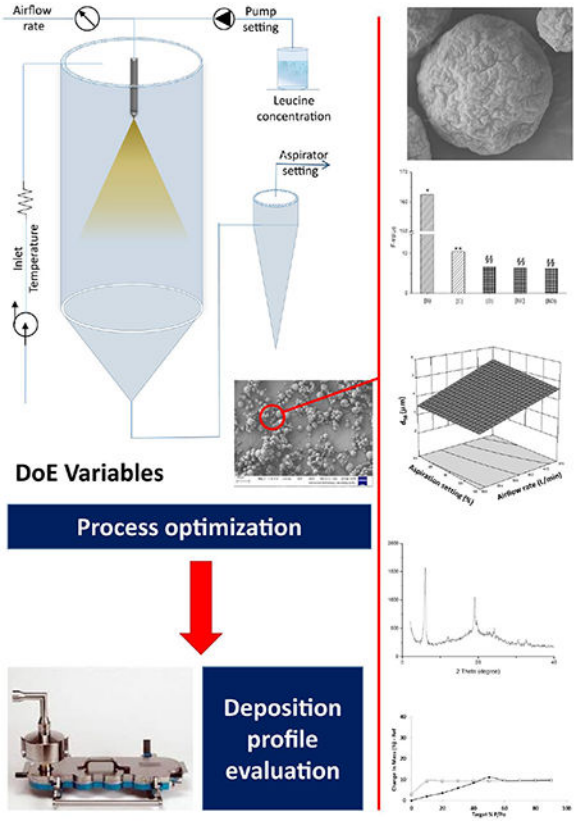

Keywords

spray drying; trehalose; leucine; design of experiments; dry powder for inhalation; pulmonary formulation; DPI

1. Introduction

Pulmonary drug delivery is an important area of research with potential to impact the treatment of lung specific diseases, such as asthma, chronic obstructive pulmonary disease (COPD) or respiratory tract infections (Chow et al., 2007; Kadota et al., 2017; Weers and Miller, 2015). Delivery to the lungs may also be employed to effect bioabsorption of small drugs or therapeutic peptides in order to obtain a systemic effect (Amaro et al., 2015a; Amaro et al., 2015b; Ógáin et al., 2011). Regardless of the desired effect, delivery devices for drug inhalation can be divided into three principal categories: nebulizers, pressurized metered-dose inhalers (pMDIs) and dry powder inhalers (DPI) (Pilcer and Amighi, 2010). Among them, DPIs continue to have an important role in delivering medicinal aerosols due to their advantages, which include – ease of handling, superior portability (compared to nebulisers), no need for propellant (unlike pMDIs), greater storage stability, higher drug payload, and the fact that they present a greater hurdle for generic competitors to enter the market (Bosquillon et al., 2001; Chen et al., 2016; Smith and Parry-Billings, 2003). Drugs

for DPI devices are formulated as powders, in which particles should be sufficiently small (aerodynamic diameter in the range of 1–5 μm) to enable lung deposition (Feng et al., 2011; Scherließ et al., 2014; Simon et al., 2016). However, such dimensions, in conjunction with other physicochemical characteristics (i.e. percentage of amorphous material, moisture content and electrostatic charging), may lead to strong particle cohesiveness as well as poor powder ability to flow through the device and to disperse in the inhaled air flow (Sou et al., 2011; Tajber et al., 2009). To overcome these drawbacks several particle engineering techniques such as spray drying, spray freeze drying, and supercritical fluid technology have been developed (Chow et al., 2007; Pilcer and Amighi, 2010). Of these, spray drying is regarded as a particle engineering technique suitable for the efficient production of inhalable particles with relatively straightforward scale-up capabilities (Pilcer and Amighi, 2010; Ziaee et al., 2017). The spray drying process consists of the atomization of a feed solution containing the drug into droplets that rapidly dry because of their high surface area and intimate contact with the heated drying gas. Evaporative cooling of the droplets reduce the temperature below that of the drying gas and the resulting dried powder is protected from overheating by rapid removal from the drying zone (Johnson, 1997a). This technology allows for accurate control of particle characteristics such as size, morphology, density, and distribution of components in the particles (Amaro et al., 2015a; Chow et al., 2007; Li et al., 2016; Weers et al., 2007). Typically a spray drying process leads to the production of an amorphous powder which may absorb atmospheric moisture, causing aggregation due to capillary forces and recrystallization. These characteristics are undesirable for inhaled powders, since the powders are physically unstable and resulting agglomerates or crystals may not be within the respirable size range (Li et al., 2016; Zhou et al., 2013), resulting in reduced lung powder deposition (Aquino et al., 2012; Li et al., 2016).

Different strategies have been proposed to increase the physical stability of the formulation, for example by inducing a crystalline form (Kumon et al., 2010), mixing different active ingredients in the same formulation, so providing physical protection from the environment of one compound by another (Zhou et al., 2014), or by using protective excipients (Chen et al., 2016). One of the most widely used protective excipients is L-leucine (Aquino et al., 2012; Feng et al., 2011; Seville et al., 2007); a number of studies have reported on the use of this amino acid with a view to improving powder dispersion and adding moisture protection to the formulation (Boraey et al., 2013; Chang et al., 2014; Li et al., 2016; Shur et al., 2008). These useful properties of L-leucine are due to its preferential precipitation on the surface of drying droplets, resulting in the formation of a hydrophobic outer shell layer. The displacement of L-leucine away from the droplet center is characteristic of a system where the ratio of the time for solute diffusion from the droplet surface to its center, to the time for droplet drying, is greater than 1 (Peclet number >1). This behavior leads to the formation of a wrinkled or raisin-like particle morphology that causes an improvement in dispersion of particles resulting in efficient drug delivery into the lower regions of the lungs (Boraey et al., 2013; Feng et al., 2011; Healy et al., 2014; Simon et al., 2016; Sou et al., 2013; Vehring, 2008).

These characteristics of leucine enable a powder with reduced cohesion to be obtained, and a “ready to use” inhalable formulation to be developed, without the need to use coarse carrier particles (usually lactose) for delivering the active pharmaceutical ingredient (API) to the

respiratory tract. In fact, most DPI formulations consist of micronized drug particles blended with larger carrier particles, typically lactose monohydrate, with the aim of enhancing powder flowability, dispersion and reducing particle agglomeration. Particles stick to the carrier particle surface by physical forces of interaction and should detach from the carrier on device actuation and powder inhalation (Simon et al., 2016). The efficiency of these types of powder formulations is highly dependent on the carrier quality, source and particle size distribution as well as the inhalation flow rate and dispersion capacity of the respective DPI device. The development of carrier-free dry powder inhaler formulations has the potential to overcome issues associated with carrier particles as a critical component of the formulation. For example blending steps are avoided (for single API formulations) and the aerosolisation properties of the formulation will depend solely on the characteristics of the API particles or API-containing particles, together with DPI inhaler performance and the patient's inhalation technique. Furthermore the limited amount of excipient included in carrier-free formulations permits the inhaled powder mass to be limited, and makes the delivery of high dose actives to the lungs possible (Healy et al., 2014).

Moreover, it has also been demonstrated that the outer layer of leucine has an anti-hygroscopic effect which protects the inner core from environmental moisture, improving the chemical and physical stability of the formulation (Chang et al., 2014).

Although a number of reports in the literature detail the use of L-leucine as an excipient for spray dried formulations (Vehring, 2015), none of these studies used a systematic approach to examine the effect of spray dryer parameters and L-leucine concentration on physical properties of the final product. Thus, in this paper, a Design of Experiment (DoE) approach has been used to systematically screen, optimize and identify the critical and non-critical process and formulation factors affecting the powder characteristics, as well as the interactions between experimental variables, for the production of a model dry powder formulation intended for lung delivery application.

We selected D-trehalose dihydrate as a model carrier agent since this material possesses properties that make it a promising carrier excipient for stabilization and protection of biomolecules (Amaro et al., 2015a; Johnson, 1997b; Maury et al., 2005).

In fact, it has been well established that trehalose is known to be a superior stabilizer in providing protection to biological materials against dehydration and desiccation, in comparison with a number of other sugars, especially during lyophilization, spray drying and exposure to high temperatures in solution (Lipiainen et al., 2018; Rajagopal et al., 2013).

It has been demonstrated by a number of different groups that this non-reducing sugar is an effective stabilizer of proteins in the amorphous state (Colaco et al., 1992; Johnson, 1997a; Maury et al., 2005). Other studies have established the protective action of trehalose on protein integrity, avoiding loss of bioactivity (López-Díez and Bone, 2004; Ógáin et al., 2011; Yoshii et al., 2008). Carpenter and Crowe (Carpenter and Crowe, 1989) suggested the water replacement theory to explain the protective action of sugar compounds on biomolecules, where the formation of hydrogen bonding between the excipient and the

biomolecule occurs when water is removed, maintaining the structural integrity of the peptide/protein.

Other sugars commonly used in the pharmaceutical industry, such as sucrose, glucose and sorbitol, do not present all the characteristics described above and these unique qualities make trehalose undoubtedly one of the most promising excipients for delivering biopharmaceutical compounds to the respiratory tract (Mensink et al., 2017).

Furthermore, trehalose is able to guarantee long-term stabilization of therapeutic proteins in the dried form, and it has been identified as one of the most suitable sugars for protecting proteins from denaturation during storage, due to the high glass transition temperature it confers (Liao et al., 2002)

Finally, trehalose is a generally recognized as safe (GRAS) material by the FDA, as it has no potential to damage the lungs and is easily cleared by metabolism (Pilcer and Amighi, 2010; Rahimpour et al., 2014).

2. Materials and methods

2.1 Materials

D-Trehalose dihydrate was purchased from PanReac AppliChem (Darmstadt, Germany); L-leucine (LL) was obtained by Sigma (Arklow, Ireland). The most relevant physical and chemical proprieties of both compounds in terms of formulations stability and spray drying feasibility are listed in Table 1. Water was purified and filtered using an Elix 3 connected to a Synergy UV system (Millipore, Nottingham, UK).

2.2 Preparation of spray-dried D-trehalose/L-leucine powder

Composite systems containing different D-trehalose and LL weight ratios (namely 70:30; 80:20 and 90:10 % w/w, trehalose/LL) were spray dried as 5% (w/v) solutions in water using a Büchi Mini Spray dryer B-290 (Flawil, Switzerland) operating in the open mode, coupled with a 0.7 mm 2 fluid nozzle and using compressed air as the drying gas in a co-current mode. Spray dried particles were separated from the drying gas by a high performance cyclone (Büchi, Flawil, Switzerland). Process parameters were set according to the requirements of the individual runs as identified in the factorial design study outlined in Section 2.9. Each formulation was stored after processing at 4°C in a desiccator containing silica gel.

2.3. Particle size distribution

Particle size distributions were determined using a Mastersizer 2000 laser diffraction instrument (Malvern Instruments, UK) with a dry powder dispersion accessory (Scirocco 2000). The dispersive air pressure was set at 3 bar and a vibration feed rate of 75% was used in order to achieve an obscuration between 0.5% and 6%. Mastersizer 2000 software was used for data evaluation. The particle size was expressed as the geometric median diameter based on a volume distribution (d_{50}), and the polydispersity of the powders was expressed by the span values:

$$Span = [d_{90} - d_{10}]/d_{50,} \quad (1)$$

where d_{90}, d_{50} and d_{10} indicate the equivalent volume diameters corresponding to the 90, 50 and 10% points of the cumulative distribution curve, respectively. The values presented are the average of three determinations.

2.4. Production yield

Yields were calculated based on the weight of powder collected expressed as a percentage of the weight introduced into the feed solution, giving the yield per cent by weight (%).

2.5. Scanning electron microscopy (SEM)

SEM micrographs of spray dried materials were acquired using a Zeiss Supra Variable Pressure Field Emission Scanning Electron Microscope (Oberkochen, Germany) equipped with a secondary electron detector. The samples were fixed on aluminum stubs using double-sided adhesive tape and sputter-coated with gold. Visualization was performed at 5 kV and photo micrographs were taken at different magnifications in more than one region of the sample.

2.6. Thermal analysis

Thermogravimetric analysis (TGA) was performed using a TGA Q50, (TA Instruments, Dublin, Ireland), to determine the amount of residual moisture content (RMC) contained in samples after spray drying. Sample weights between 4 and 8 mg were used and placed into open aluminum pans; a temperature range of 25–150 °C was employed with a heating rate of 10°C/min and the RMC was defined as the weight loss between 25 and 120 °C. The values presented are the average of three analyses.

Modulated differential scanning calorimetry measurements were carried out under nitrogen purge using a MDSC Q2000 instrument (TA Instruments, Dublin, Ireland). Powder samples (2–4 mg) were placed in aluminum pans (40 μl), sealed, and heated over the temperature range of 0 to 130 °C. The modulation parameters chosen to ensure separation of reversing and non-reversing events were 0.8 °C/ 60 s at a ramp rate of 5 °C/min. The values reported represent an average of three analyses. Both TGA and MDSC systems were controlled by Q Advantage software (version 5.5, TA Instruments, Dublin, Ireland).

2.7. Dynamic vapor sorption (DVS)

Water sorption kinetic profiles were obtained using a DVS (Advantage, Surface Measurement Systems, Alperton, UK) at 25.0 ± 0.1 °C. Water was used as the probe vapor. Samples were dried at 0% relative humidity (RH) for 1 h and then subjected to step changes of 10% RH up to 90% RH, and the reverse for desorption. The sample mass was allowed to reach equilibrium, defined as dm/dt ≤ 0.002 mg/min over 10 min, before the RH was changed. Sample weights were between 15 and 20 mg.

2.8. Powder X-ray diffraction

Powder X-ray analysis was performed using a Miniflex II Rigaku diffractometer (The Woodlands, TX, USA) with Ni-filtered Cu Kα radiation (1.54 Å). The tube voltage and tube current used were 30 kV and 15 mA, respectively. The PXRD patterns were recorded (n=3) for 2 theta ranging from 5° to 40° at a step scan rate of 0.05° per second. Rigaku Peak Integral software was used to determine peak intensity for each sample using the Sonneveld-Visser background edit procedure.

2.9 In vitro aerosol deposition studies using the Next Generation Impactor (NGI)

The pulmonary deposition of the spray dried powders was estimated *in vitro* using a Next Generation Impactor (NGI, Copley Scientific Limited, UK) operated according to European Pharmacopoeial conditions (Pharmacopoeia, 2014) . The flow rate was adjusted to achieve a pressure drop of 4 kPa in the dry powder inhaler (Low resistance RS01, Plastiape, Osnago, Italy) and the time of aspiration was adjusted to obtain 4 L of air flow. NGI stages (stages 1–7 and micro-orifice collector) were coated with 1 mL silicon oil (DMPS, obtained from Sigma, Arklow, Ireland) and weighed before and after every deposition study using a precision balance (Sartorius Quintix 513-1S, Goettingen, Germany). The dry powder inhaler was loaded with a no. 3 HPMC capsules loaded with 10 mg of powder for each formulation test and the amount of deposited powder on each stage was determined gravimetrically after allowing deposition from three separate capsules for each formulation.

Deposition profiles for each formulation were determined in triplicate and the results presented are the average results of the replicated analyses. The total weight of particles with aerodynamic diameters smaller than 5 and 3 μm was calculated by interpolation from the inverse of the standard normal cumulative mass distribution less than stated size cut-off against the natural logarithm of the cut-off diameter of the respective stages (Simon et al., 2016). These amounts were considered the fine particle fraction (FPF) below 5 μm and 3 μm, and expressed as a percentage of the emitted recovered dose (ERD). The ERD was calculated from the sum of powder recovered in the NGI stages, since the use of the gravimetric method does not enable the amount of powder deposited on the NGI mouthpiece or throat to be measured. The mass median aerodynamic diameter (MMAD) of the powder was determined from the same plot, and is the particle size corresponding to the 50% point of the cumulative distribution. The geometric standard deviation (GSD) was calculated from Equation (2):

$$GSD = \sqrt{Size\ X / Size\ Y} \quad (2)$$

where X is the particle size corresponding to the 84% point and size Y is the particle size corresponding to the 16% point of the cumulative distribution (Amaro et al., 2011; Bosquillon et al., 2001).

2.10. Experimental design

A response surface randomized full factorial design (using Design Expert software, version. 10.0.1.0; Stat- Ease Inc., Minneapolis, MN, USA) was devised to assess the effect of spray

drying process parameters on particle size (d_{50} and d_{90}), span, powder yield, RMC, process outlet temperature (T_{out}) and glass transition temperature (T_g). The parameters chosen to be studied were: (A) inlet temperature (T_{in}), (B) spray dryer airflow rate, (C) pump setting (feed solution flow rate), (D) aspirator setting and (E) LL concentration. Each factor was studied at three levels: low, medium and high and each variable was assigned as −1, 0, +1 (Table 2).

The settings for all the process parameters were based on preliminary one-factor-at-a-time studies where inlet temperature was varied between 120 and 160 °C (representing the lower temperature limit to achieve a proper particle drying process and the upper limit to ensure thermal degradation of the formulation ingredients was minimized, respectively), spray dryer airflow rate from 470 to 600 liter/hours, pump setting from 5 to 20%; aspirator setting from 80 to 100% and LL concentration from 10% to 30% of the total solute content (t.s.c.) in the feed solution. The chosen factorial model was represented by:

$$Y_i = \beta_0 + \beta_1 A + \beta_2 B + \beta_3 C + \beta_4 D + \beta_5 E + \beta_{12} AB + \beta_{13} AC + \ldots \quad (4)$$

Where β_0 is the intercept, $\beta_{n\neq 0}$ is the coefficient associated with factor, n, and the letters, A, B, C, etc., represent the factors (the spray drying parameters) in the model. Combinations of factors (such as AB) represent an interaction between the individual factors in that term. In this study only main effects and two-factor interactions were considered as the most likely to influence the response and only they constituted the statistical model.

Statistical analysis of variance, ANOVA, was performed to determine the significance (p-value) and impact (F-value) of each main factor as well as their interactions. Parameters found to be significant at least the 95% confidence level were considered in the final prediction models.

3. Results and discussion

Here we implemented a factorial design approach to investigate systematically the effect of five parameters (inlet temperature, spray dryer airflow rate, pump setting, aspirator setting and LL concentration) on powder characteristics. This statistical method facilitated the identification of the most significant factors influencing the quality of the formulation (Sou et al., 2011). Results showed that the model is able to predict the response for d_{50}, d_{90}, yield, RMC and T_{out} (p value <0.0001, 0.0015, 0.0154, 0.0464, and <0.0001 respectively; a summary of result data obtained is presented in Table 3) whereas a lack of model significance was obtained for T_g and span values. The intercept and the coefficient associated with each main factor and main factor interactions are shown in Table 4.

3.1. Particle size distribution and morphology

All spray dried powders showed a monomodal particle size distribution. The median particle size was in the range 2.87–5.65 μm and the relative span value was within the range 1.75–2.62. Largest particles were obtained for sample TFD 17 (spray dried with LL content and pump setting on the highest levels and airflow rate and aspiration setting at the lowest

values) and smallest particles were found for TFD 22 (airflow rate, aspirator pump setting on the highest levels and LL content and pump setting at the lowest values).

ANOVA indicated that three of the main effects (airflow rate, pump setting and aspirator setting) and 2 two-level interactions can be regarded as impacting on the median particle size. The coefficients of the equation (from the general form of Eq. (2)) that relate the particle size to the process variables are given in Table 4. The greatest influence is found for airflow rate ($p < 0.0001$), as seen in Fig. 1A, where an increase in gas pressure in the nozzle resulted in decreased particle size. This trend is commonly known, and has been previously observed (Chawla et al., 1994; Stahl et al., 2002), and is related to the increased energy available for breaking up the liquid jet by the nozzle, thus forming smaller particles during atomization (Dean, 1987). Another important parameter identified as influencing particle size is the pump rate ($p = 0.0056$). In this case a positive coefficient was obtained in the model equation. The value suggests that an increase in spray solution feed rate (pump setting) results in larger particle size. In fact, increasing the feed flow rate provides more fluid for dispersion per unit of energy available for atomization and, as a consequence, it leads to the formation of larger spray droplets and consequently bigger particles (Amaro et al., 2011; Maury et al., 2005). The last factor found to influence the d_{50} is the aspiration setting ($p = 0.0207$). Generally this parameter is not related to the particle size distribution; however, in this case the effect could be related to an increase in the degree of aerosolization of the solution caused by the suction forces produced by aspiration, as previously described by Tajber and collaborators (Tajber et al., 2009). Analysis of variance revealed two relationships between the factors, namely airflow rate and aspiration setting (BD, $p = 0.0242$) and airflow rate and LL concentration (BE, $p = 0.0235$). Fig. 2A shows a response surface plot for the interaction BD: smaller particles can be obtained if both of the parameters are at highest levels. Nevertheless it is clear that the aspirator setting has a lesser importance in comparison with the profound impact of the airflow on particle size. In the case of the BE interaction, again an inverse correlation between the airflow rate and particle size distribution is observed but, interestingly, a slight increase in d_{50} with higher LL concentration is also revealed (Fig. 2B). This behavior can be explained by the relatively low water solubility of LL. In fact a higher concentration in the feed solution provides for a faster attainment of LL supersaturation in the drying droplet, and hence rapid precipitation occurs. Newly formed LL crystals exhibit lower mobility and tend to remain on the external surface of the droplet leading to the formation of large and hollow particles (Hoe et al., 2014).

Only the main variables were found to influence d_{90} and no factor interactions were found (Fig. 1B). d_{90} values ranged between 6.19 and 13.17 μm and, even in this case, the most influencing factor is the airflow rate ($p < 0.0001$), followed by LL concentration and the feed flow rate ($p = 0.0023$ and $p = 0.0092$, respectively). Surprisingly the coefficient related to LL concentration has a positive value; this result is in contrast with results presented by other authors, since usually an increase in LL content is coupled with better powder dispersibility and lower cohesiveness, two characteristics that are well-known to decrease d_{90} (Aquino et al., 2012; Boraey et al., 2013; Rahimpour et al., 2014). It would seem that, in this particular case, d_{90} is not related to the particle propensity to form agglomerates, since the size distribution plots were essentially monomodal (Fig. 3) The positive relationship

between LL concentration and d_{90} is more likely to be as a consequence of the tendency for LL to precipitate relatively quickly at the drying droplet surface, leading to the production of large and hollow particles when used at high concentrations, as described above.

Fig. 4 depicts the morphology of three representative formulations (namely TFD 22, TFD18 and TFD17) to show the effect of LL concentration on particle shape. The morphology of the spray dried particles changed, as expected, from solid spheres to hollow irregular particles with thin shells with increasing LL mass fraction. Using 30% of LL concentration the fraction of hollow, thin walled particles increased, becoming the most prevalent morphology type. The irregular morphology of the particle is a consequence of the tendency of the LL to precipitate on the surface of the droplet during the drying event. At the highest LL concentration, particles containing large void space are more likely to be produced, rather than dense and homogenous microspheres. The fate of the partially hollow particles depends on the thickness and mechanical properties of the shell surrounding them and, accordingly, they may eventually collapse or wrinkle (Vehring, 2008), as shown in Fig. 4C. An increase in trehalose concentration reduces this effect and, consequently, formulations containing a lower amount of LL displayed a more spherical and regular shape. It has been previously demonstrated that morphologies of the type observed in Fig 4C do not represent an obstacle in terms of powder flow and dispersibility. It has been shown that this irregular structure may, in fact, result in improved dispersion behaviour of the powder from a DPI, since particles have reduced inter-particulate contact points, and hence lower cohesive or adhesive forces than more regular-shaped/smoother particles. At the same time, such particles have an increased shape factor (X), which leads to a reduction in their aerodynamic diameter (Chen et al., 2016).

Furthermore an increase in geometric particle diameter with increasing LL mass fraction was also clearly visible, especially when comparing formulations containing 20% and 30% of LL mass fraction. A difference in span values was also noted for the different batches. The values obtained were 1.79 ± 0.16, 1.76 ± 0.02 and 2.03 ± 0.13 for batches TFD22, TFD8 and TFD17 (corresponding to formulations containing 10%, 20% and 30% of LL in mass fraction respectively). Results clearly show that TFD22 and TFD8 values do not differ significantly from one other (Fig.3 and table 1s), but the span value of TFD 17 is higher. This finding is confirmed by SEM analysis, where large particles are mostly visible in fig. 4C compared to fig. 4A and 4B. Thus, the size distribution of TFD 17 is wider in comparison to the other two batches and the particle population is observed to be less homogeneous.

3.2. Yield

The weights of the powders collected after each spray drying run were expressed as the percent of the initial amount of the solids taken for solution preparation. The lowest yield achieved was for sample TFD 20 (53% of the starting amount) and the largest was for TFD29 (~81%). A trend between the results of the thermogravimetric analysis and the yields recovered was seen (Fig. 5A). Although the R^2 value is low, in general, greater amounts of product were recovered when the powders had a lower RMC. This result may be associated with the highly cohesive nature of the powder containing a higher amount of water (Tajber et

al., 2009). Droplets emerging from the two-fluid nozzle tend to be projected in the direction of the drying chamber vertical wall; if droplet/particle drying has proceeded insufficiently before impacting with the wall, the particles can adhere, resulting in the formation of a wet deposit and hence a reduced powder yield (Maury et al., 2005).

A weak relationship between T_{out} and product yield was also obtained: on increasing T_{out}, a progressively drier product is obtained. This indicates that sufficient droplet/particle drying occurs before impact with the wall of the drying chamber and the extent of wall deposition is reduced resulting in progressive improvement in yield (Fig. 5B). It is interesting to note that both yield and T_{out} are affected by T_{in} and it is not surprising that inlet temperature had the greatest (positive) influence among the spray drying process parameters on the recovered yield ($p = 0.0071$, Fig 1C).

Fig. 1C also shows that airflow rate and solution feed rate have a positive and negative effect respectively on the product yield. The airflow rate ($p = 0.0079$) affects the particle size, with higher airflow leading to smaller particles, as described in section 3.1. Usually a low d_{50} is linked to low yield when a laboratory scale spray drier is used, as it has been demonstrated that larger particles have an increased likelihood of being retained in the cyclone then smaller ones (Maa et al., 1998; Stahl et al., 2002). In the present study this general observation was contradicted since an inverse correlation between the yield and median particle size values was observed, as depicted in Fig. 5C. However, in this study a high efficiency cyclone has been used and thus this result can be partially explained by better ability of the high efficiency cyclone to trap a greater proportion of smaller particles in comparison with the standard cyclone (Amaro et al., 2011). Another reason for the observed trend of lower d_{50} relating to higher yield may be attributed to the larger specific surface area (SSA) characterizing smaller particles, and consequently the higher contact between the drying air and the particle surface. This scenario results in better drying conditions and hence a powder with reduced stickiness and with a lower tendency to adhere to the walls of either the drying chamber or the cyclone separator before reaching the collection vessel.

However, the effect of airflow rate on the recovery yield should be studied in more depth since only a slight correlation between d_{50} and RMC was found (Fig. 5D). Furthermore, the airflow rate is not one of the main parameters that statistically affects the RMC of the formulations (Fig. 1D) and its effect on product yield should be further investigated.

The negative coefficient associated with pump setting ($P = 0.0239$) means that yield is inversely related to the amount of feed solution flowing through the nozzle. As well as the airflow rate, this parameter is statistically linked to the median particle size and consequently the specific surface area of the powder: higher pump rate value results in higher d_{50} and lower SSA. A higher pump setting could hinder proper powder drying and thus increase particle adhesiveness.

The only interaction observed was between airflow rate and T_{in}, with a p-value of 0.0136 (Fig. 2C). Although p and F values achieved were lower in comparison with the single parameters, there is a synergy between the variables that affects the product yield, i.e. the variables statistically influenced one another.

3.3 Residual moisture content

Residual moisture content is a key parameter that influences physical stability of an amorphous spray dried powder. Generally, the level of moisture affects particle size and excipient crystallization during long-term storage due to plasticization of the amorphous phase, thereby deteriorating the dispersion performance of the powder as well as its airway deposition profile (Maa et al., 1998).

Measurement of loss on drying by TGA showed moisture content of powders between 1.47 and 6.06%. These results, as previously described for production yield, were examined in the context of their association with outlet temperature. We found that a weak inverse relationship is present, as shown in Fig. 5E. The trend observed implies that higher outlet values result in lower residual solvent; this correlation has also been discerned by other authors (Billon et al., 2000; Stahl et al., 2002). The relationship between RMC and the main factors was obtained after transformation of the final linear equation to an inverse square root equation in order to reach the best statistical description of the parameters affecting the response. In this case a positive coefficient associated with a variable has a negative effect on the output and vice versa. It was found that RMC was significantly affected by solution flow rate (C), inlet temperature (A) and their reciprocal interaction ($p = 0.0020$, 0.0159 and 0.0467 respectively): generally powders produced with the highest air temperature and lowest feed flow rate resulted in the driest formulations. Obviously, on increasing inlet temperature, more energy is supplied to the drying chamber and hence a more efficient solvent removal results (Amaro et al., 2011), whereas a high pump setting generates more solvent vapor and reduces the exhaust temperature leading to less efficient drying (Maury et al., 2005). However, the pump setting effect is prominent only on powders containing the higher LL amount, as revealed by the statistically significant relationship between these two factors (Fig. 2D). The effect may be explained by the addition of LL below a certain value (~ 12% w/w of t.s.c. as shown by the bottom graph projection in Fig. 2D), which does not allow the critical concentration for shell formation to be reached as the droplet evaporation progresses during the spray-drying process. On the other hand, an enrichment in LL content leads to the production of an outer impermeable structure which hinders the movement of moisture from the particle core, resulting in a higher RMC (Aquino et al., 2012; Vehring, 2008).

3.4 Outlet temperature

The outlet temperature of a spray drying process is a result of various factors including those related to the apparatus used and material being processed (Tajber et al., 2009). In this study, the outlet temperatures varied between 52 and 97 °C. It has been found that this response was primarily dictated by inlet temperature, as expected, followed by the feed solution flow rate (both $p < 0.0001$, Fig. 1E). Indeed the greater the solution flow rate, the more liquid is supplied to the drying chamber and more solvent vapor is generated, therefore decreasing the exhaust temperature and increasing the RH at the outlet (Amaro et al., 2011). The other parameter with an influence on the resulting T_{out} was the aspiration setting. T_{out} increased with increasing aspirator capacity: a lower drying air flow rate causes an increase in product residence time in the drying chamber leading to a greater degree of moisture removal and

thus a decrease in outlet temperature. For the purpose of this study, a high outlet temperature is desirable in order to obtain drier powders and higher yields, as described above (Fig. 2).

3.5 Thermal properties

All spray dried formulations were characterized by amorphous trehalose and crystalline leucine with T_g varying between 45 and 80° C as measured by DSC (data not shown), and no obvious trends were seen between T_g onsets and factorial outputs. The glass transition temperature of fully amorphous dry trehalose is 117 °C as reported in the literature (Jain and Roy, 2009; Simon et al., 2016); the reduced values in this case can be ascribed to the RMC within the powder since water acts as a potent plasticizer for sugar glasses (Hancock and Zografi, 1994). The inverse relationship between RMC and formulations T_g is depicted in Fig. 5F.

3.6. Water vapor sorption and desorption isotherms of powders

DVS was used to evaluate the effect of moisture on the solid-state stability of the powders. For this experiment only one representative formulation for each LL concentration level was examined: TFD22, TFD8 and TFD17 (corresponding to LL concentration levels −1,0 and +1 respectively). TFD 22 and TFD8 (Fig. 6A and B) showed similar profiles: both were characterized by the presence of an open hysteresis loop, their sorption isotherms presented an inflection point at ~50% and ~60% RH respectively reaching about 10% mass increment of their initial weight at 90% RH. Desorption curves are characterized by no mass change until 10% RH and a final moisture uptake of approximately 3%. These events are believed to occur as a result of amorphous trehalose collapsing into its crystalline stable form (Amaro et al., 2015a), with the crystallization being signaled by a mass loss in the DVS sorption profile since the crystalline form has a lower affinity for water than the amorphous form. XRPD confirmed this assumption, since characteristic peaks of crystalline trehalose dihydrate (Raimi-Abraham et al., 2014) were identified in the sample after DVS analysis (Fig. 7 A and B).

Interestingly TFD17 (LL concentration level +1) was able to sorb approximately 37% of its weight in moisture at 90% RH but the change in mass at the end of the cycle was near 0%. These observations indicate that the water sorption behavior was reversible and no moisture-induced trehalose recrystallization occurred (Fig 6C), as confirmed by XRPD data where only crystalline LL characteristic peaks were found after the DVS run (Fig. 7C). This result may be explained by the fact that, while the water sorption was extensive, presumably due to the small particle size and high surface area of the spray dried material, water was adsorbed only onto the outer surface of particles, and was poorly absorbed into the amorphous regions of the composite system as a consequence of the barrier effect of LL. Thus the trehalose was protected from crystallization. This effect was also observed to a lesser extent in TFD8 formulation where a delay in recrystallization (from 50% RH of TFD22 to 60% RH) was seen, as well as the presence of low intensity crystalline peaks in PXRD pattern after the DVS run, indicating only partially recrystallized sample. However, in this case (TFD8) the LL concentration is not sufficient to protect the powder against moisture and a higher concentration of LL should be used, as mentioned above.

3.7 In vitro aerosol deposition studies

The Next Generation Impactor (NGI) was used to assess the aerodynamic performance of the spray-dried powders mentioned in section 3.6 using a low resistance RS01 Plastiape dry powder inhaler device. The amount of powder in each stage was determined gravimetrically. The total emitted dose value depicts only the amount of powder recovered from stage 1 to the micro-orifice collector (MOC) since it was not experimentally feasible to obtain the measurement of the powder weight in the NGI mouthpiece and 'throat'. All formulations investigated in this part of the study demonstrated a favorable deposition profile, as detailed in table 5. TFD17 (LL concentration +1) showed less powder deposition in stages with cut off diameters less than 3 μm (after stage 3), whereas a reduction in LL from 30% to 10% led to a higher FPF as well as lower MMAD value (Fig.8 and Table 5). These results were unexpected since they differ from other studies where a decrease in MMAD is generally associated with an increase in LL mass fraction due to reduced particle density and cohesiveness (Feng et al., 2011; Simon et al., 2016).A possible explanation for this unusual deposition behavior could be related to the geometric particle size. In fact, the median particle size, d_{50}, is directly proportional to LL concentration in the examined formulations. A higher LL content leads to a larger geometric particle size and results in reduced fraction of particles depositing in the lower stages of the NGI. Nevertheless these powder flowing characteristics could be associated to the different process input used by other authors and further studies are needed.

4. Conclusion

This paper highlights the potential for rational particle engineering by establishing an understanding of the interplay between process parameters during spray drying. Results suggest that models constructed could be used to optimize the spray drying process for the production of powders with suitable characteristics for pulmonary delivery, and the model may be adopted to optimize formulations of therapeutic peptides or proteins, as well as small molecules, for the treatment of lung disease. In this respect, the DoE approach has enabled the exploration of a wide range of conditions in an efficient manner, while also enabling interactions to be explored.

The DoE highlighted a number of interesting results. For example, the interaction between feed flow rate and LL concentration is shown to affect the drying process of the droplets, and the effect of the feed flow rate is revealed only after a certain lower level of LL is exceeded. Furthermore, it has been shown that the outlet temperature is a function, not of single or multiple individual parameter(s) but, once again, it depends also on the interaction between LL concentration and the feed flow rate. These results may be useful, especially in formulating relatively unstable APIs which require strictly controlled conditions for processing and storage.

In addition, results indicate that an increase in LL concentration led to the production of larger particles, in contrast with the established theories, according to which an increase in LL concentration within a formulation should lead to a reduced particle size, as a consequence of reduced cohesiveness. Moreover, this unusual result is consistent with the inverse correlation between product yield and d_{50}, in contrast with the norms in the

literature, where more usually, a lower d_{50} corresponds to a lower yield. For this particular system, geometric particle size results for collected spray dried powder may be attributed to the production of larger non-agglomerated particles at higher LL concentrations, which are not lost to the spray dryer filter.

Finally, results indicate that LL mass ratio impacted the physical stability of the powder against environmental humidity: a high LL concentration protected amorphous trehalose from moisture-induced crystallization but, on the other hand, an excessive amount of this amino acid (30% w/w) could hinder the deposition performance of the formulation, suggesting that a balance needs to be found between physical stability and deposition characteristics for this system.

Although in some cases it is difficult to compare outcomes for different spray dryers, this paper describes trends in how the input parameters influence the characteristics of a powder, and such trends should be readily transferred to pilot scale or industrial scale spray drying units.

In conclusion, we note that the present study focused on the characteristics of formulations stored for a limited period of time in an environment with controlled humidity and temperature. Further experiments are necessary to understand in more detail the impact of process variables on the medium-to-long term physical and chemical stability of trehalose/leucine based formulations.

Supplementary Material

Refer to Web version on PubMed Central for supplementary material.

Acknowledgement

Research reported in this publication was supported by the National Heart, Lung And Blood Institute of the National Institutes of Health under Award Numbers P01HL128191 and R01HL080414. The content is solely the responsibility of the authors and does not necessarily represent the official views of the National Institutes of Health.

6. References

Amaro MI, Tajber L, Corrigan OI, Healy AM, 2011 Optimisation of spray drying process conditions for sugar nanoporous microparticles (NPMPs) intended for inhalation. International Journal of Pharmaceutics 421, 99–109. [PubMed: 21963473]

Amaro MI, Tajber L, Corrigan OI, Healy AM, 2015a Co-spray dried carbohydrate microparticles: crystallisation delay/inhibition and improved aerosolization characteristics through the incorporation of hydroxypropyl-beta-cyclodextrin with amorphous raffinose or trehalose. Pharm Res 32, 180–195. [PubMed: 25074469]

Amaro MI, Tewes F, Gobbo O, Tajber L, Corrigan OI, Ehrhardt C, Healy AM, 2015b Formulation, stability and pharmacokinetics of sugar-based salmon calcitonin-loaded nanoporous/nanoparticulate microparticles (NPMPs) for inhalation. International Journal of Pharmaceutics 483, 6–18. [PubMed: 25660067]

Aquino RP, Prota L, Auriemma G, Santoro A, Mencherini T, Colombo G, Russo P, 2012 Dry powder inhalers of gentamicin and leucine: formulation parameters, aerosol performance and in vitro toxicity on CuFi1 cells. International Journal of Pharmaceutics 426, 100–107. [PubMed: 22301426]

Billon A, Bataille B, Cassanas G, Jacob M, 2000 Development of spray-dried acetaminophen microparticles using experimental designs. International Journal of Pharmaceutics 203, 159–168. [PubMed: 10967438]

Boraey MA, Hoe S, Sharif H, Miller DP, Lechuga-Ballesteros D, Vehring R, 2013 Improvement of the dispersibility of spray-dried budesonide powders using leucine in an ethanol–water cosolvent system. Powder Technology 236, 171–178.

Bosquillon C, Lombry C, Preat V, Vanbever R, 2001 Influence of formulation excipients and physical characteristics of inhalation dry powders on their aerosolization performance. J Control Release 70, 329–339. [PubMed: 11182203]

Carpenter JF, Crowe JH, 1989 An infrared spectroscopic study of the interactions of carbohydrates with dried proteins. Biochemistry 28, 3916–3922. [PubMed: 2526652]

Chang Y-X, Yang J-J, Pan R-L, Chang Q, Liao Y-H, 2014 Anti-hygroscopic effect of leucine on spray-dried herbal extract powders. Powder Technology 266, 388–395.

Chawla A, Taylor KMG, Newton JM, Johnson MCR, 1994 Production of spray dried salbutamol sulphate for use in dry powder aerosol formulation. International Journal of Pharmaceutics 108, 233–240.

Chen L, Okuda T, Lu X-Y, Chan H-K, 2016 Amorphous powders for inhalation drug delivery. Advanced drug delivery reviews 100, 102–115. [PubMed: 26780404]

Chow AHL, Tong HHY, Chattopadhyay P, Shekunov BY, 2007 Particle Engineering for Pulmonary Drug Delivery. Pharmaceutical Research 24, 411–437. [PubMed: 17245651]

Colaco C, Sen S, Thangavelu M, Pinder S, Roser B, 1992 Extraordinary stability of enzymes dried in trehalose: simplified molecular biology. Bio/technology (Nature Publishing Company) 10, 1007–1011.

Dean CJK, 1987 Spray Drying Handbook, Fourth Edition By Masters K, Halstead Press, New York, 1985, 696 pp. AIChE Journal 33, 172-173.

Feng AL, Boraey MA, Gwin MA, Finlay PR, Kuehl PJ, Vehring R, 2011 Mechanistic models facilitate efficient development of leucine containing microparticles for pulmonary drug delivery. International Journal of Pharmaceutics 409, 156–163. [PubMed: 21356284]

Hancock BC, Zografi G, 1994 The relationship between the glass transition temperature and the water content of amorphous pharmaceutical solids. Pharm Res 11, 471–477. [PubMed: 8058600]

Healy AM, Amaro MI, Paluch KJ, Tajber L, 2014 Dry powders for oral inhalation free of lactose carrier particles. Advanced drug delivery reviews 75, 32–52. [PubMed: 24735676]

Hoe S, Ivey JW, Boraey MA, Shamsaddini-Shahrbabak A, Javaheri E, Matinkhoo S, Finlay WH, Vehring R, 2014 Use of a Fundamental Approach to Spray-Drying Formulation Design to Facilitate the Development of Multi-Component Dry Powder Aerosols for Respiratory Drug Delivery. Pharmaceutical Research 31, 449–465. [PubMed: 23974958]

Jain NK, Roy I, 2009 Effect of trehalose on protein structure. Protein Science 18, 24–36. [PubMed: 19177348]

Johnson KA, 1997a Preparation of peptide and protein powders for inhalation. Advanced drug delivery reviews 26, 3–15. [PubMed: 10837528]

Johnson KA, 1997b Preparation of peptide and protein powders for inhalation. Advanced drug delivery reviews 26, 3–15. [PubMed: 10837528]

Kadota K, Senda A, Tagishi H, Ayorinde JO, Tozuka Y, 2017 Evaluation of highly branched cyclic dextrin in inhalable particles of combined antibiotics for the pulmonary delivery of anti-tuberculosis drugs. International Journal of Pharmaceutics 517, 8–18. [PubMed: 27913241]

Kumon M, Kwok PCL, Adi H, Heng D, Chan H-K, 2010 Can low-dose combination products for inhalation be formulated in single crystalline particles? European Journal of Pharmaceutical Sciences 40, 16–24. [PubMed: 20172026]

Li L, Sun S, Parumasivam T, Denman JA, Gengenbach T, Tang P, Mao S, Chan H-K, 2016 I-Leucine as an excipient against moisture on in vitro aerosolization performances of highly hygroscopic spray-dried powders. European Journal of Pharmaceutics and Biopharmaceutics 102, 132–141. [PubMed: 26970252]

Liao YH, Brown MB, Nazir T, Quader A, Martin GP, 2002 Effects of sucrose and trehalose on the preservation of the native structure of spray-dried lysozyme. Pharm Res 19, 1847–1853. [PubMed: 12523664]

Lipiainen T, Raikkonen H, Kolu AM, Peltoniemi M, Juppo A, 2018 Comparison of melibiose and trehalose as stabilising excipients for spray-dried beta-galactosidase formulations. Int J Pharm 543, 21–28. [PubMed: 29567196]

López-Díez EC, Bone S, 2004 The interaction of trypsin with trehalose: an investigation of protein preservation mechanisms. Biochimica et Biophysica Acta (BBA) - General Subjects 1673, 139–148. [PubMed: 15279885]

Maa Y-F, Nguyen P-A, Andya JD, Dasovich N, Sweeney TD, Shire SJ, Hsu CC, 1998 Effect of Spray Drying and Subsequent Processing Conditions on Residual Moisture Content and Physical/Biochemical Stability of Protein Inhalation Powders. Pharmaceutical Research 15, 768–775. [PubMed: 9619788]

Maury M, Murphy K, Kumar S, Shi L, Lee G, 2005 Effects of process variables on the powder yield of spray-dried trehalose on a laboratory spray-dryer. European Journal of Pharmaceutics and Biopharmaceutics 59, 565–573. [PubMed: 15760738]

Mensink MA, Frijlink HW, van der Voort Maarschalk K, Hinrichs WLJ, 2017 How sugars protect proteins in the solid state and during drying (review): Mechanisms of stabilization in relation to stress conditions. Eur J Pharm Biopharm 114, 288–295. [PubMed: 28189621]

Ógáin ON, Li J, Tajber L, Corrigan OI, Healy AM, 2011 Particle engineering of materials for oral inhalation by dry powder inhalers. I—Particles of sugar excipients (trehalose and raffinose) for protein delivery. International Journal of Pharmaceutics 405, 23–35. [PubMed: 21129458]

Pharmacopoeia E, 2014 Preparations for Inhalation: Aerodynamic Assessment of Fine Particles, in: Community E (Ed.), European Pharmacopoeia, 9th ed Council of Europe, Strasbourg, pp. 276–286.

Pilcer G, Amighi K, 2010 Formulation strategy and use of excipients in pulmonary drug delivery. International Journal of Pharmaceutics 392, 1–19. [PubMed: 20223286]

Rahimpour Y, Kouhsoltani M, Hamishehkar H, 2014 Alternative carriers in dry powder inhaler formulations. Drug Discovery Today 19, 618–626. [PubMed: 24269834]

Raimi-Abraham BT, Moffat JG, Belton PS, Barker SA, Craig DQM, 2014 Generation and Characterization of Standardized Forms of Trehalose Dihydrate and Their Associated Solid-State Behavior. Crystal Growth & Design 14, 4955–4967.

Rajagopal K, Wood J, Tran B, Patapoff TW, Nivaggioli T, 2013 Trehalose Limits BSA Aggregation in Spray-Dried Formulations at High Temperatures: Implications in Preparing Polymer Implants for Long-Term Protein Delivery. Journal of Pharmaceutical Sciences 102, 2655–2666. [PubMed: 23754501]

Scherließ R, Ajmera A, Dennis M, Carroll MW, Altrichter J, Silman NJ, Scholz M, Kemter K, Marriott AC, 2014 Induction of protective immunity against H1N1 influenza A(H1N1)pdm09 with spray-dried and electron-beam sterilised vaccines in non-human primates. Vaccine 32, 2231–2240. [PubMed: 24631078]

Seville PC, Learoyd TP, Li HY, Williamson IJ, Birchall JC, 2007 Amino acid-modified spray-dried powders with enhanced aerosolisation properties for pulmonary drug delivery. Powder Technology 178, 40–50.

Shur J, Nevell TG, Ewen RJ, Price R, Smith A, Barbu E, Conway JH, Carroll MP, Shute JK, Smith JR, 2008 Cospray-dried unfractionated heparin with L-leucine as a dry powder inhaler mucolytic for cystic fibrosis therapy. Journal of Pharmaceutical Sciences 97, 4857–4868. [PubMed: 18351636]

Simon A, Amaro MI, Cabral LM, Healy AM, de Sousa VP, 2016 Development of a novel dry powder inhalation formulation for the delivery of rivastigmine hydrogen tartrate. International Journal of Pharmaceutics 501, 124–138. [PubMed: 26836711]

Smith IJ, Parry-Billings M, 2003 The inhalers of the future? A review of dry powder devices on the market today. Pulmonary Pharmacology & Therapeutics 16, 79–95. [PubMed: 12670777]

Sou T, Kaminskas LM, Nguyen T-H, Carlberg R, McIntosh MP, Morton DAV, 2013 The effect of amino acid excipients on morphology and solid-state properties of multi-component spray-dried

formulations for pulmonary delivery of biomacromolecules. European Journal of Pharmaceutics and Biopharmaceutics 83, 234–243. [PubMed: 23183447]

Sou T, Orlando L, McIntosh MP, Kaminskas LM, Morton DAV, 2011 Investigating the interactions of amino acid components on a mannitol-based spray-dried powder formulation for pulmonary delivery: A design of experiment approach. International Journal of Pharmaceutics 421, 220–229. [PubMed: 21963471]

Stahl K, Claesson M, Lilliehorn P, Linden H, Backstrom K, 2002 The effect of process variables on the degradation and physical properties of spray dried insulin intended for inhalation. Int J Pharm 233, 227–237. [PubMed: 11897427]

Tajber L, Corrigan OI, Healy AM, 2009 Spray drying of budesonide, formoterol fumarate and their composites-ll. Statistical factorial design and in vitro deposition properties. International journal of pharmaceutics 367, 86–96. [PubMed: 18929634]

Vehring R, 2008 Pharmaceutical Particle Engineering via Spray Drying. Pharmaceutical Research 25, 999–1022. [PubMed: 18040761]

Vehring R, 2015 Theoretical Tools for Particle Engineers: Spray Drying Complex Formulations for Inhalation. Respiratory Drug Delivery Europe 1, 187–196.

Weers JG, Miller DP, 2015 Formulation Design of Dry Powders for Inhalation. Journal of Pharmaceutical Sciences 104, 3259–3288. [PubMed: 26296055]

Weers JG, Tarara TE, Clark AR, 2007 Design of fine particles for pulmonary drug delivery. Expert Opinion on Drug Delivery 4, 297–313. [PubMed: 17489656]

Yoshii H, Buche F, Takeuchi N, Terrol C, Ohgawara M, Furuta T, 2008 Effects of protein on retention of ADH enzyme activity encapsulated in trehalose matrices by spray drying. Journal of Food Engineering 87, 34–39.

Zhou Q, Gengenbach T, Denman JA, Yu HH, Li J, Chan HK, 2014 Synergistic Antibiotic Combination Powders of Colistin and Rifampicin Provide High Aerosolization Efficiency and Moisture Protection. The AAPS Journal 16, 37–47. [PubMed: 24129586]

Zhou Q, Morton DAV, Yu HH, Jacob J, Wang J, Li J, Chan HK, 2013 Colistin Powders with High Aerosolisation Efficiency for Respiratory Infection: Preparation and In Vitro Evaluation. Journal of Pharmaceutical Sciences 102, 3736–3747. [PubMed: 23904207]

Ziaee A, Albadarin AB, Padrela L, Faucher A, O'Reilly E, Walker G, 2017 Spray drying ternary amorphous solid dispersions of ibuprofen – An investigation into critical formulation and processing parameters. European Journal of Pharmaceutics and Biopharmaceutics 120, 43–51. [PubMed: 28822874]

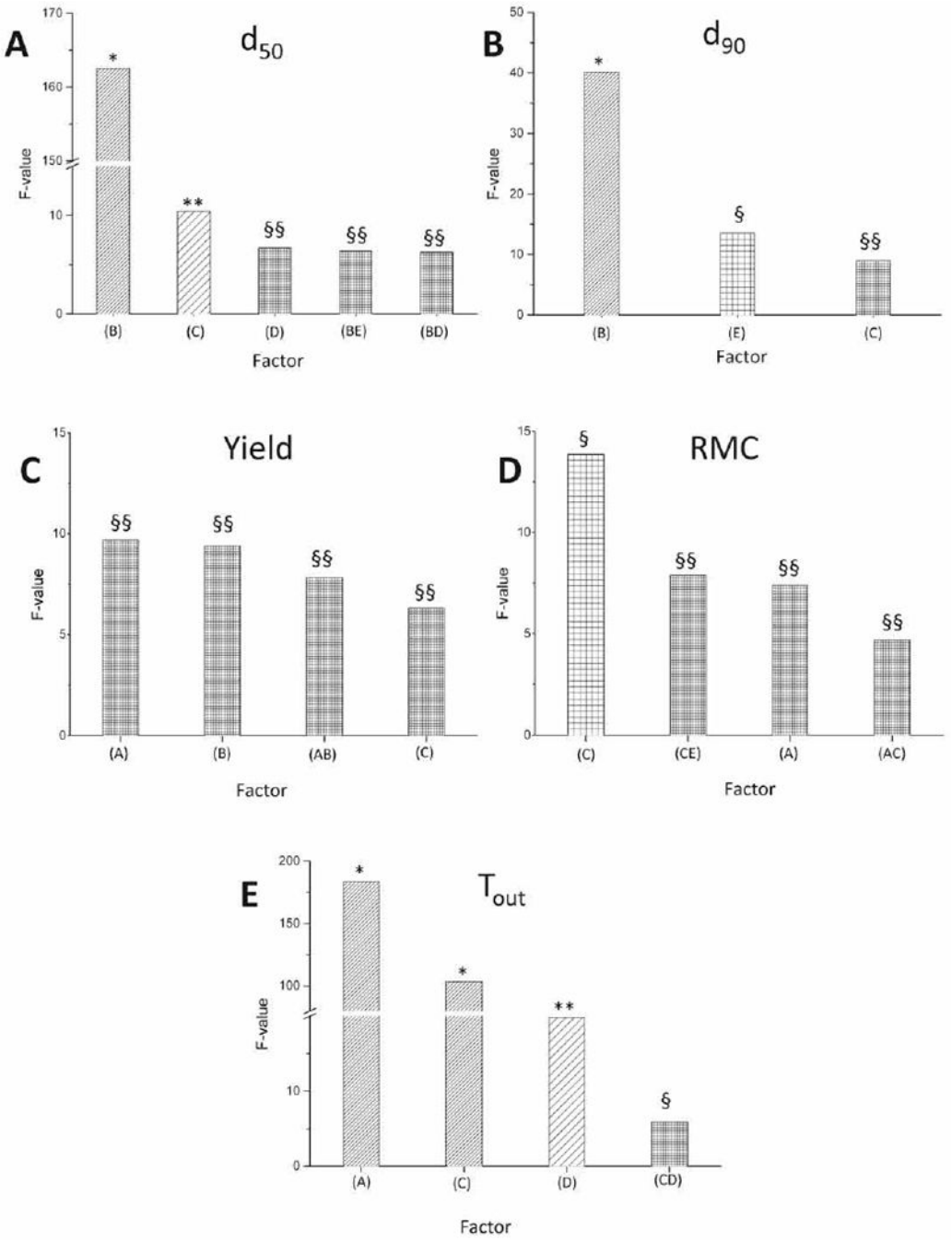

Fig. 1.

Bar plots showing F-value and associated p-value determining statistical significance of the main effects and interactions for the response: A, d_{50}; B, d_{90}; C, yield; D, RMC; E, T_{out}. Only terms with p-values equal to or less than 0.05 were plotted. *, $p<0.0001$; **, $p<0.001$; §, $p<0.005$; §§, $p<0.05$. Factors: (A), T_{in}; (B), airflow rate; (C), pump setting; (D), aspiration setting; (E), LL concentration.

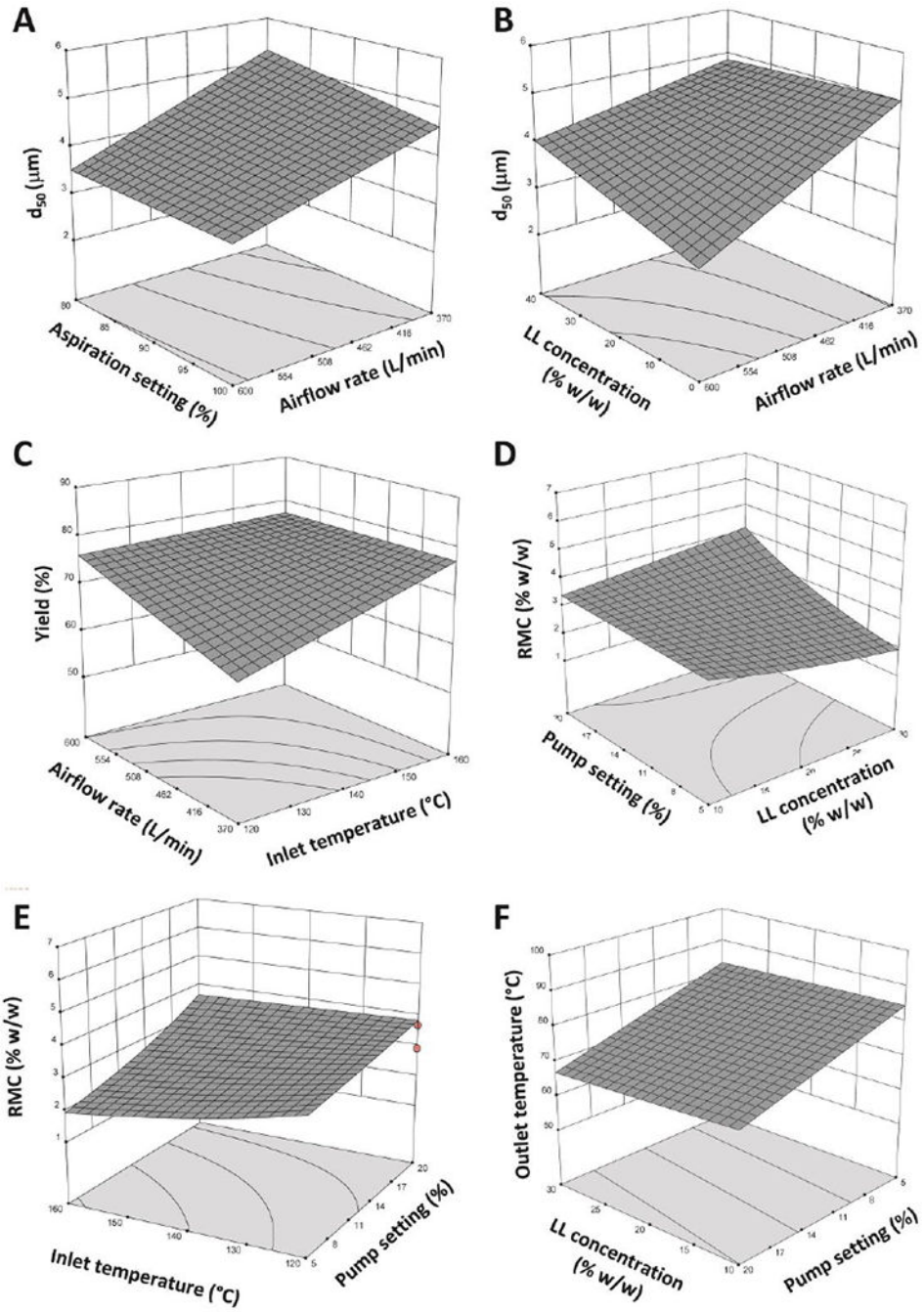

Fig.2.

Response surface plots showing the effects of the two main parameters having the greatest influence on the given response.

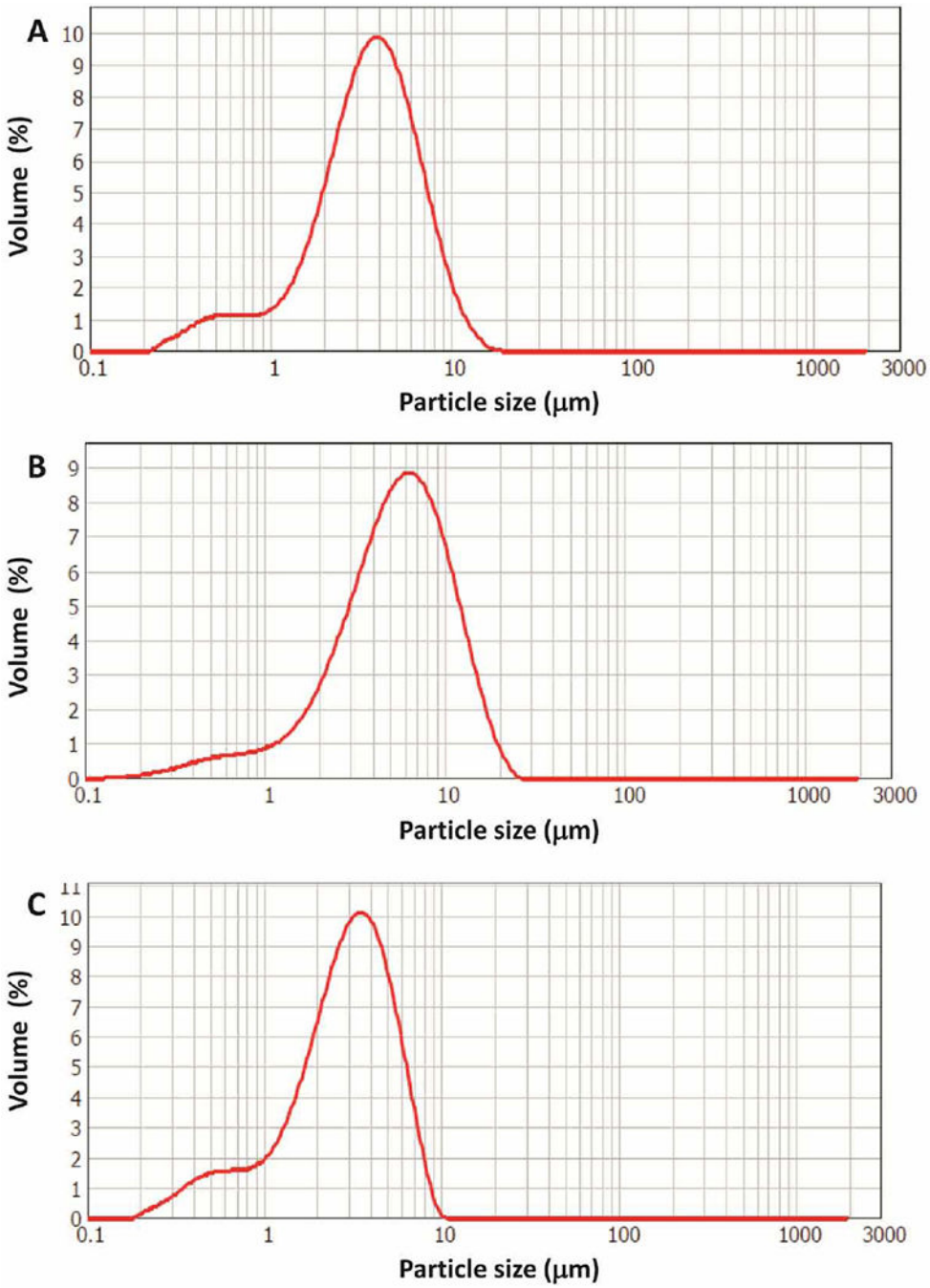

Fig.3.

Volumetric particle size distribution of formulations: A) TFD22; B) TFD8 and C) TFD17. d_{50}, d_{90}, d_{10} and span values are shown in table 1s.

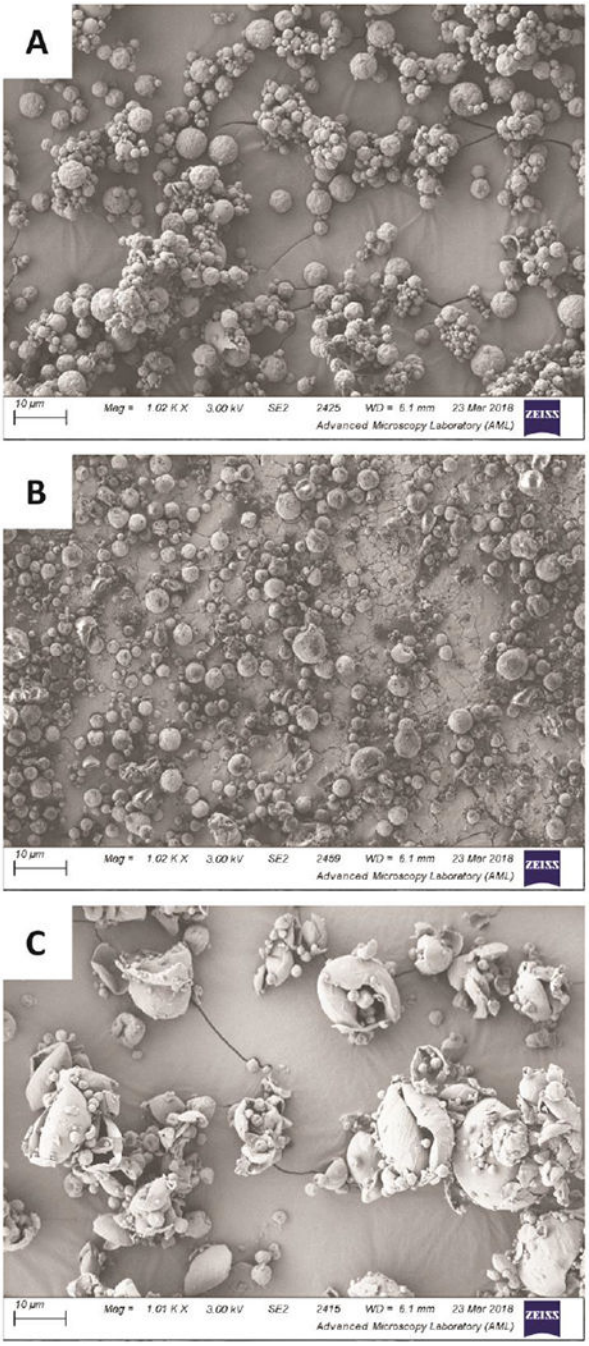

Fig.4.

SEM micrographs of: A) formulation TFD22 (10% LL concentration); B) formulation TFD8 (20% LL concentration); C) TFD 17 (30% LL concentration)

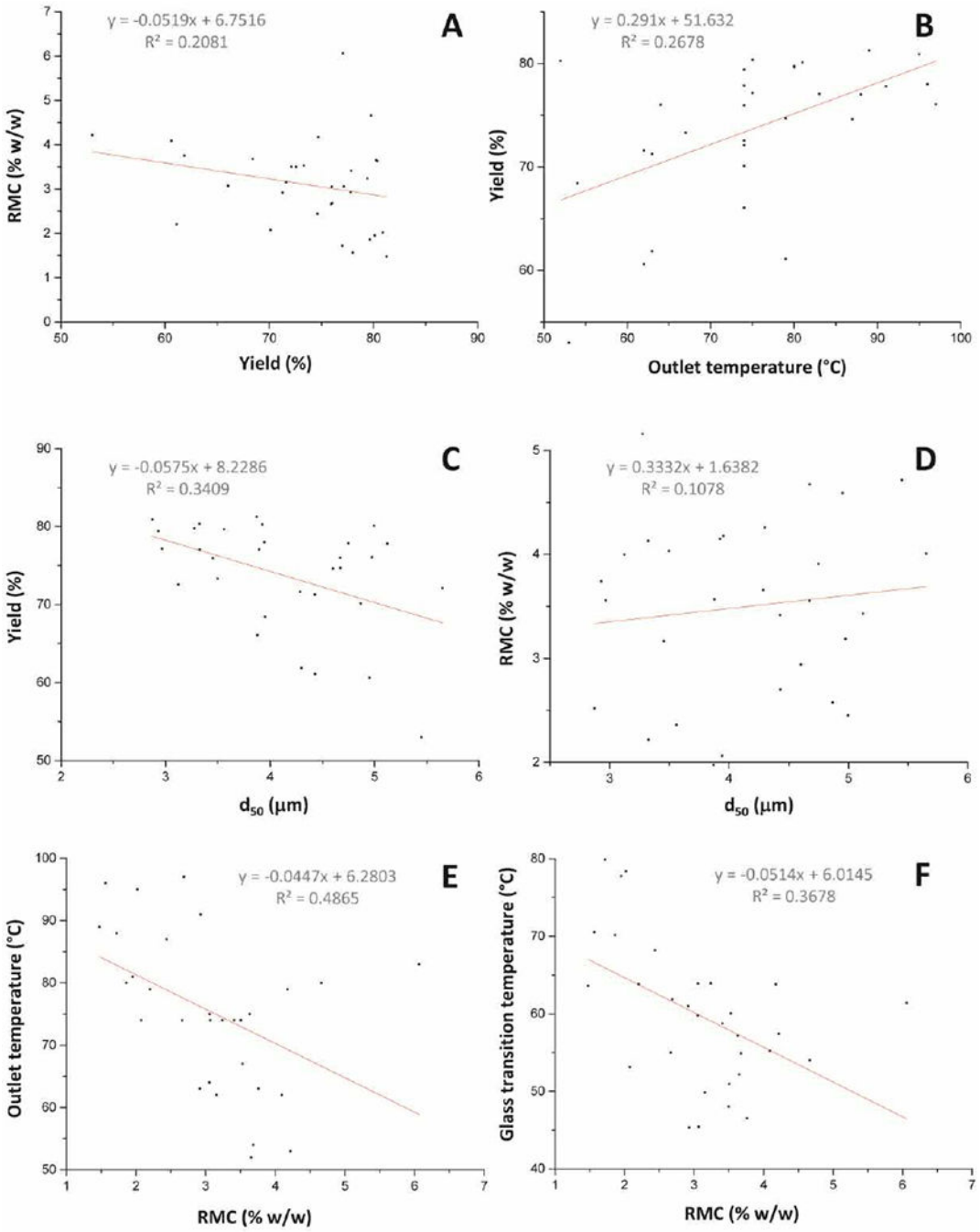

Fig. 5.

Relationships between: A) RMC and yield, B) yield and T_{out}; C) yield and d_{50}; D) RMC and yield; E) T_{out} and RMC; F) T_g and RMC.

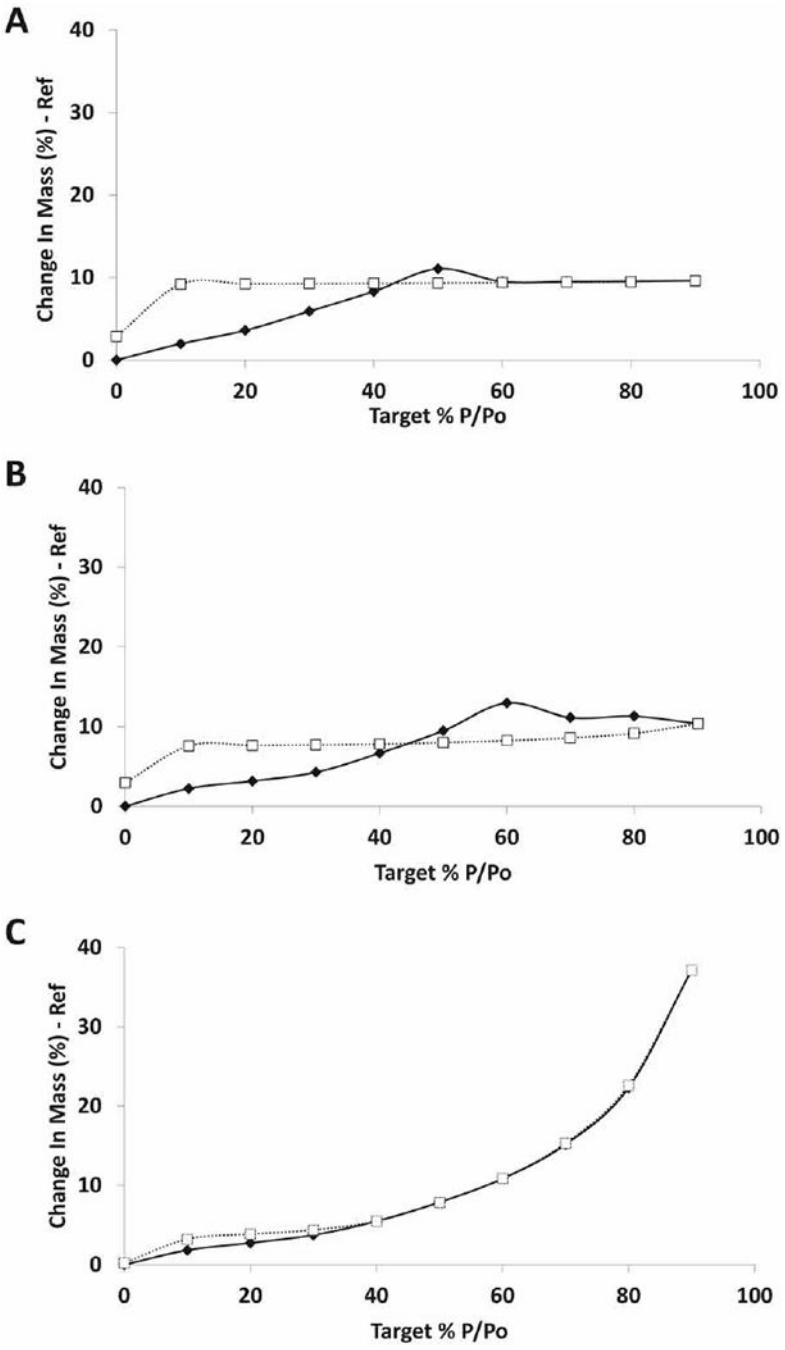

Fig.6.

Water vapor sorption and desorption isotherms of formulations: A) TFD22; B) TFD8 and C) TFD17. Solid line: sorption isotherm; dotted line: desorption isotherm.

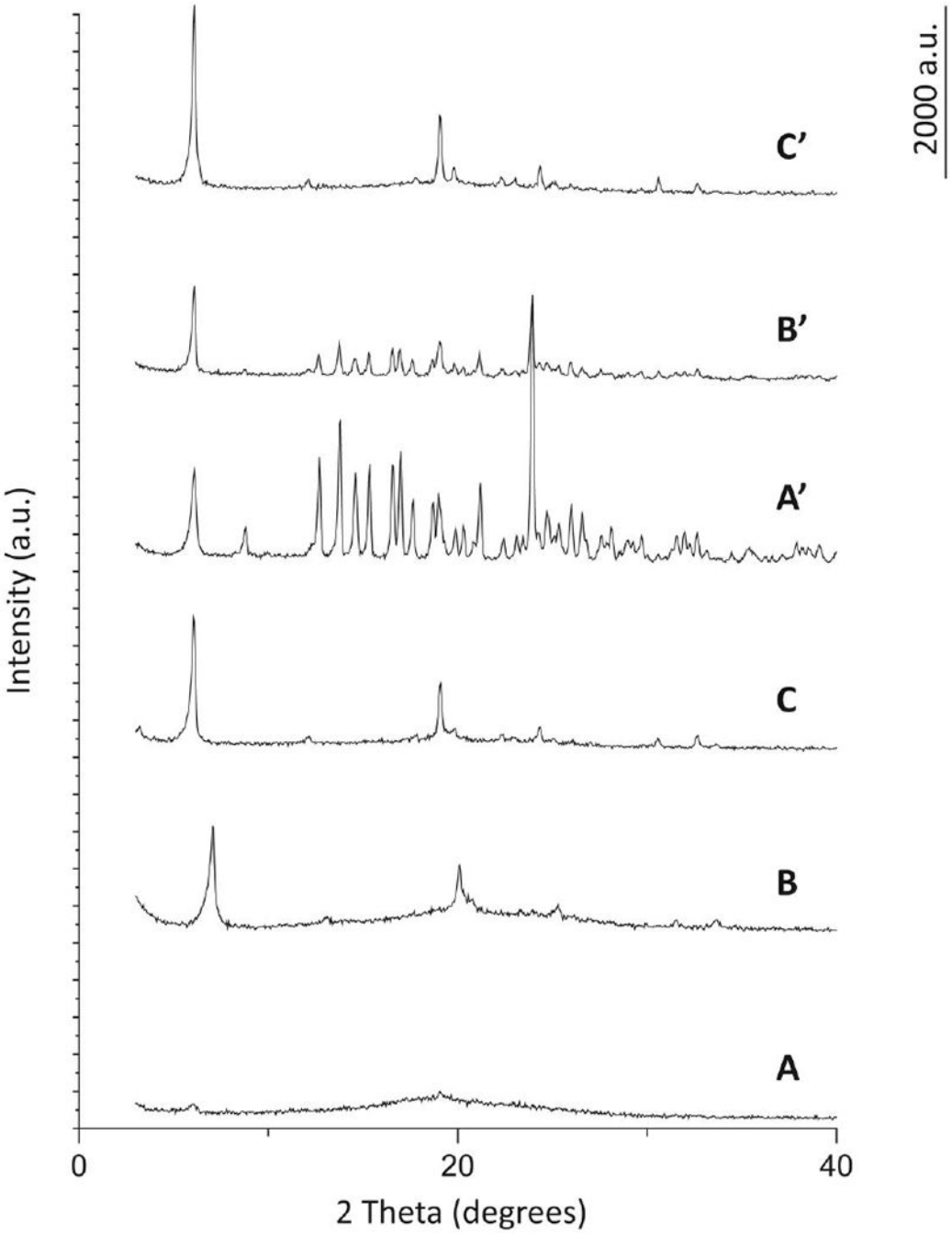

Fig. 7.

XRPD diffractograms of formulations TFD22 pre (A) and post (A') DVS analysis; TFD8 pre (B) and post (B') DVS analysis and TFD17 pre (C) and post (C') DVS analysis.

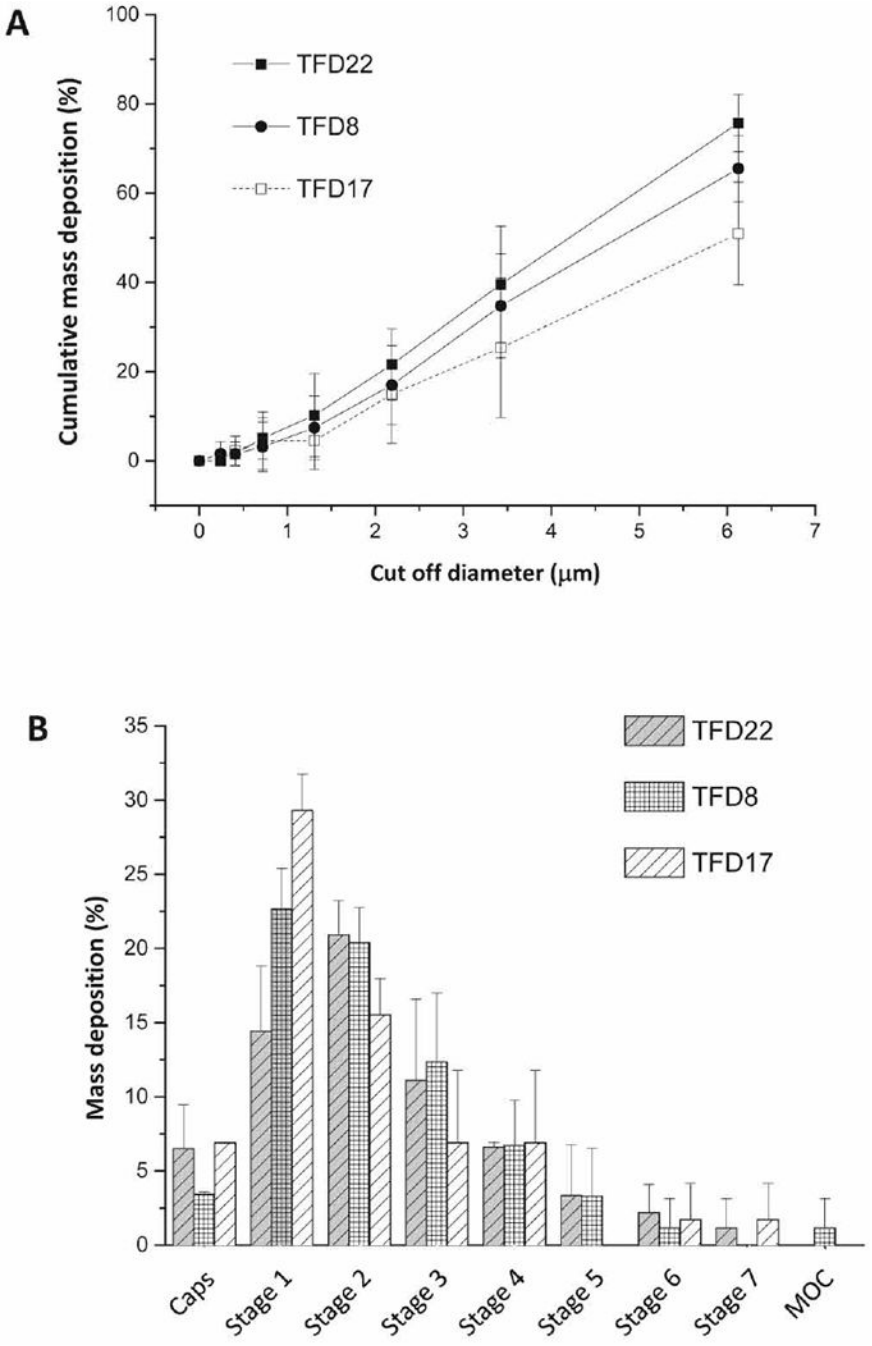

Fig.8.

Cumulative mass deposition percentage, A, and NGI stage mass deposition profile, B, of formulations TFD8, TFD17 and TFD22. MOC: micro-orifice collector

Table 1

Trehalose and L-leucine physical and chemical characteristics

Compound	Solubility in water at 25°C (g/100 ml)	T_g(°C)	Melting point (°C)	Molecular weight (g/mol)
Trehalose	68.9	*117*	203	342.23
L-leucine	*2.15*	*140*	*293*	*131.18*

Table 2

Processing variables used in the factorial study

Parameter	Low (−1)	Medium (0)	High (+1)	Units
(A) inlet temperature	120	140	160	°C
(B) airflow rate	470	535	600	L/h
(C) pump setting	5	10	20	%
(D) aspirator setting	80	90	10	%
(E) LL concentration	10	20	30	% (w/w)

Table 3

Design matrix and the responses from the analyses

Formulation ID	Variable terms					Responses				
	T_{in}	airflow rate	pump setting	aspirator setting	LL conc.	d_{50} (μm)	d_{90} (μm)	Yield (%)	RMC (%)	T_{out} (°C)
TFD1	−1	+1	+1	−1	+1	3.92	9.66	80.2	3.7	52
TFD2	−1	0	0	−1	0	4.29	9.76	71.6	3.2	62
TFD3	0	0	−1	0	−1	4.67	9.73	74.7	4.3	79
TFD4	+1	+1	+1	−1	−1	3.12	6.44	72.5	3.6	74
TFD5	−1	+1	−1	+1	+1	4.95	13.17	60.6	5.1	62
TFD6	0	0	+1	0	−1	3.28	6.89	79.7	4.8	80
TFD7	−1	−1	+1	0	0	3.32	7.38	80.3	3.8	75
TFD8	−1	+1	0	0	0	3.95	8.93	68.4	3.8	54
TFD9	+1	+1	+1	+1	+1	3.89	9.74	77.0	6.8	83
TFD10	−1	−1	−1	+1	−1	4.75	9.79	77.8	3.5	74
TFD11	+1	−1	−1	−1	−1	4.97	10.25	76.0	2.8	97
TFD12	−1	0	0	−1	0	4.29	9.49	61.8	4.2	63
TFD13	0	−1	−1	+1	0	5.12	11.06	77.8	3.5	91
TFD14	−1	−1	+1	+1	+1	3.45	8.20	75.9	2.7	74
TFD15	−1	−1	−1	−1	+1	4.86	11.45	70.1	2.1	74
TFD16	0	0	0	+1	+1	3.88	8.92	66.0	3.1	74
TFD17	+1	+1	−1	−1	+1	5.65	12.57	72.1	3.6	74
TFD18	−1	−1	+1	−1	−1	2.93	6.22	79.4	3.3	74
TFD19	−1	+1	+1	+1	−1	3.50	7.56	73.3	3.6	67
TFD20	−1	+1	−1	−1	−1	5.45	11.38	53.0	4.3	53
TFD21	−1	−1	−1	+1	+1	4.43	9.68	61.1	2.2	79
TFD22	+1	−1	+1	+1	−1	2.87	6.51	80.9	2.1	95
TFD23	0	0	0	+1	+1	3.56	9.56	79.6	1.9	80
TFD24	0	0	+1	0	−1	2.97	6.19	77.1	3.1	75
TFD25	+1	−1	+1	−1	+1	3.33	8.80	77.0	1.7	88
TFD26	+1	+1	−1	+1	−1	4.60	9.89	74.6	2.5	87
TFD27	0	+1	0	−1	0	4.67	12.79	76.0	3.1	64
TFD28	+1	−1	0	0	+1	3.94	9.87	78.0	1.6	96
TFD29	+1	0	−1	+1	+1	3.87	8.90	81.2	1.5	89
TFD30	0	0	−1	0	−1	4.99	10.99	80.1	2.0	81
TFD31	−1	+1	0	0	0	4.43	12.79	71.2	3.0	63

Table 4

Coefficients equations linking the spray drying parameters (in terms of coded factors) with responses on predictable parameters. R^2 values are given to indicate the goodness of fit of the theoretical models to the experimental values.

Term	d_{50} (μm)	d_{90} (μm)	Yield (%)	RMC (%)[a]	T_{out} (°C)
Intercept	*4.14*	*9.56*	*74.17*	*3.13*	*76.21*
A	*−0.088*	*−0.27*	*3.21*	*−0.28*	*10.29*
B	*−0.77*	*−1.54*	*3.19*	*0.28*	*−0.89*
C	*0.19*	*0.72*	*−2.60*	*0.60*	*−7.75*
D	*−0.16*	*−0.33*	*1.23*	*0.030*	*3.42*
E	*0.092*	*0.87*	*−0.30*	*−0.14*	*−1.08*
AB	*0.030*	*0.26*	*−3.26*	*0.27*	*−0.92*
AC	*0.047*	*−0.18*	*0.43*	*0.35*	*0.20*
AD	*0.088*	*−0.21*	*0.56*	*−0.041*	*−0.44*
AE	*0.031*	*−0.018*	*0.44*	*0.20*	*−0.51*
BC	*0.030*	*−0.14*	*1.82*	*0.35*	*0.94*
BD	*0.017*	*0.28*	*−1.31*	*0.096*	*0.34*
BE	*0.16*	*0.38*	*0.66*	*0.19*	*−0.41*
CD	*0.013*	*−0.21*	*−0.48*	*0.14*	*2.06*
CE	*0.11*	*0.33*	*0.56*	*0.52*	*−0.40*
DE	*−0.086*	*−0.22*	*−2.16*	*0.24*	*−0.27*
R^2	0.9360	0.8373	*0.7620*	*0.7103*	*0.9586*

[a]The values contributing to this response has been transformed (inverse square root transformation) prior to the statistical analysis

Table 5

Summary of deposition properties of NGI tested powders

Formulation	MMAD (μm)	GSD	FPF < 3μm (%)	FPF <5 μm (%)
TFD8	5.25 ± 1.01	4.33 ± 1.35	44.3 ± 7.99	58.4 ± 7.26
TFD17	6.45 ± 0.21	4.55 ± 1.56	44.6 ± 6.52	53.9 ± 7.32
TFD22	3.97 ± 0.54	3.62 ± 0.97	54.3 ± 4.07	68.5 ± 1.63